



# Experimental and Numerical Analysis of Lightweight Hybrid Composites Under Low Velocity Impact

Kumar Maharshi<sup>1</sup> · Shivdayal Patel<sup>1</sup>

Received: 7 March 2024 / Accepted: 29 April 2024 / Published online: 23 May 2024  
© The Author(s), under exclusive licence to Springer Nature B.V. 2024

## Abstract

The experimental and numerical study of Jute—Basalt hybrid composites was performed under low-velocity impact (LVI) considering the low cost and higher specific strength and stiffness. Hybrid composites were fabricated using the vacuum infusion method to improve fiber volume fraction to reduce the air defect. The LVI tests were conducted on the Instron 9350 model at three impacting energies of 10 J, 20 J, and 30 J to study the impact force, absorbed energy, maximum displacement, and damaged area. The failure behaviour of impact-tested specimens of the natural fiber composites obtained from CT Scan was validated by three-dimensional numerical modelling using the VUMAT subroutine in ABAQUS/Explicit. The experimental and numerical results showed that the peak force and absorbed energy were significantly improved and adding basalt fabric enhanced the peak performance of jute composite. The simulation results helped to understand the delamination phenomenon which was not visible in the samples after the test. Experimental results were validated with numerical simulation results considering the 10, 20, and 30 J energy level. The peak force of B-JFRP was improved due to hybridization and the damage resistance of it could be seen as the impactor was unable to perforate at 30 J fully. The alternating stacking sequence helped in minimizing the use of basalt fabric and enhanced the overall performance of the hybrid composite. Biodegradable hybrid natural fiber composites are a promising category for developing lightweight and impact-resistant structural materials for marine applications, wind turbine, and defense industry applications.

**Keywords** Composites · Hybrid composite · Low velocity impact · Natural Fiber

## 1 Introduction

The improvement in composite structures with new and innovative approach to enhance their capabilities and utility in areas of marine applications, aerospace, automobile, sports and military have found many usages with natural fiber composites and its hybrid [1, 2]. Natural fibers are eco-friendly and biodegradable such as jute fibers which have

---

✉ Shivdayal Patel  
shivdayal@iiitdmj.ac.in

<sup>1</sup> Mechanical Engineering Department, Indian Institute of Information Technology Design and Manufacturing, Jabalpur, Madhya Pradesh 482005, India

high specific strength and stiffness to weight ratio, acting as an important parameter while designing a composite material [1–5]. Therefore, to understand their mechanical behaviour, especially when loaded under static or fatigue conditions where they exhibit relatively brittle behaviour with extensive matrix cracking and delamination leading to stiffness degradation and load-carrying ability, it becomes necessary to investigate the material properties under such conditions [2–4]. Jute fiber composite have high stiffness [5, 6], fatigue, thermal stability and wear capability among other natural fibers. It displayed biodegradability and compatibility among other natural fibers and epoxies to develop the impact resistant natural fiber composite [5–7]. Ramesh et al. [7] studied the prospects of hybridisation with improved strength and modulus including bending strength.

Basalt is a naturally occurring igneous rock whose fibers are par supreme than glass fibers in many aspects. Its usage has caught attention in many important industries including aerospace and automobile industries, household applications and usage with other natural fibers has impacted natural fiber composites to a great extent [8, 9]. Amuthakkannan et al. [10, 11] performed the experimental study for fabrication of the hybrid (jute and basalt) composite for different fiber weight percentage and stacking sequence. The natural fiber hybrid composite materials with wear resistance properties for marine applications were evaluated by Fiore et al. [12, 13]. The interlaminar shear and tensile properties for fiber metal hybrid jute-basalt composite sandwich structures were studied by Zareei et al. [14]. Various mechanical properties were evaluated by Lopresto et al. [15] and were compared with glass fiber composites where 35–42% increase in Young's modulus as well as better compressive strength and flexural behaviour were seen. The viability and intra and interlaminar properties of commercially available basalt fiber was characterised by Scalici et al. [16] utilising two different fabrication process of resin transfer method where the intralaminar properties were found better in VARIM due to better wetting of the fibers and interlaminar properties were better received in hand impregnated vacuum bagging process. Basalt fiber have also found to enhance various mechanical properties of synthetic fibers through hybridisation such as stiffness of glass fiber composite [17], impact, flexural and interlaminar shear properties of flax fiber composite [18], low and high velocity impact responses of homogenous and hybrid composites [19–23].

Development, fabrication and modelling of thin composite laminates under low velocity were an important area where barely visible impact damage (BVID) or micro cracks become a critical factor [20, 21]. Such modelling helped to understand how matrix cracking, delamination, fiber failure and other damage phenomenon were happening during impact and it also saved time and cost of physical testing [19–27]. There have been many attempts to fabricate and mechanically characterise the composite material but few have attempted to include the low velocity assessment of the same [23, 28–30]. Few attempts have been made to understand the failure of natural fiber composite under impact [31, 32].

Rajole et al. [29] studied the ballistic performance of jute epoxy composite and also using rubber as core material by varying the thickness and impacting velocities. The results obtained experimentally showed that increasing thickness enhanced the energy absorption capacity of the composite and reduced the residual velocity. The study performed on the use of basalt fiber for hybridisation in glass fiber composite to assess the impact response and post impact flexural properties for four different configurations including pure glass and basalt fiber composites was studied by Sarasini et al. [30] showing most favourable damage resistance by intercalated composite and high energy absorption due to basalt fiber. The same study was further extended to aramid fiber as well with similar results. Bandaru et al. [22, 23] performed experimental and numerical investigation of the basalt fiber hybridisation on 3D angle-interlock fabric of Kevlar polypropylene composite

for LVI showing peak force for basalt due to its stiffness while hybrid absorbed the most energy due to the elastic nature of Kevlar. Above literature showed that the very limited work was performed for the low velocity impact analysis of hybrid jute –basalt composite using experimental study.

The jute-basalt hybrid composite was fabricated using the vacuum infusion method with alternating stacking sequences to determine the damage resistance of multidirectional polymer matrix composite laminated plates subjected to a drop-weight impact event (ASTM D7136 standard). The composite panels were tested for impact resistance using an Instron 9350 drop weight impact tester at three different energy levels: 10 J, 20 J and 30 J. The alternating stacking sequence was found to be significant during peak force and impact energy in B-JFRP. Partial perforation was observed at 30 J impact which is a good indicator of high stiffness and strength. The hybrid composite was able to recover without much damage, indicating good bonding between the fibers and matrix. To verify the experimental results and identify modes of failure of fiber and matrix, a numerical approach was taken by developing a model of the same composite in ABAQUS/Explicit using VUMAT subroutine. The numerical model was validated with experimental results tested in low velocity impact. The numerical results were compared with the experimental results in terms of impact force, energy absorption, maximum displacement and damaged area for different energy levels. The same parameters were also compared with basalt fabric composite to understand the benefits and advantages of hybridization. The hybrid jute basalt composites were found to be light weight, impact resistant, biodegradable and eco-friendly, making them suitable for automotive and defence industry applications.

## 2 Materials and Method of Fabrication

In the present study, for the fabrication of hybrid composite, Jute and Basalt fabric materials of plain weave of areal density  $240 \text{ g/m}^2$  and  $220 \text{ g/m}^2$  were purchased from the Vardhman Fancy Stores, Ambala, Haryana and the Vruksha Composites, Chennai, Tamil Nadu, respectively. For the binding of the hybrid composite, low viscosity epoxy resin of  $1100 \text{ kg/m}^3$  was procured from CF Composites, New Delhi. These fabrics were plain weave and considered as transversely isotropic material in 1- and 2- directions. Laminates were fabricated using Vacuum Infusion Method (VIM) [5, 6] where stacks of fabric were laid on the acrylic board and sealed, and a mixture of epoxy (LY556) and hardener (HY 917) in a ratio of 10:1 was flown through the pipes under vacuum as shown in Fig. 1. Panels were left to set within the setup for 48 h before demoulding and then placed in oven at  $50^\circ\text{C}$  overnight to remove any excess moisture. The calculated fiber volume fraction of hybrid composite was 43.22% where Jute and basalt contributed 31.9% and 11.32%, respectively. The samples were finally cut using Abrasive water jet machine (AWJM) as per the ASTM standard D7136 [31].

The composite laminates were made in standard stacking sequence  $[(+45^\circ/-45^\circ)/(0^\circ/90^\circ)]_{NS}$  [31] from jute and basalt fabrics and alternate stacking was taken for hybrid composite laminate based on the study by Amuthakkannan et al. [10, 11] where they observed better impact and strength properties using the alternate stacking sequence. Both composite laminates had different number of layers of fabric in order to achieve a prescribed thickness of around 5 mm as per the standard. The composite plates were made in rectangular shape of 150 mm by 100 mm as shown in Figs. 2 and 3 panels each were cut from a bigger panel using AWJM to have consistency during the test.

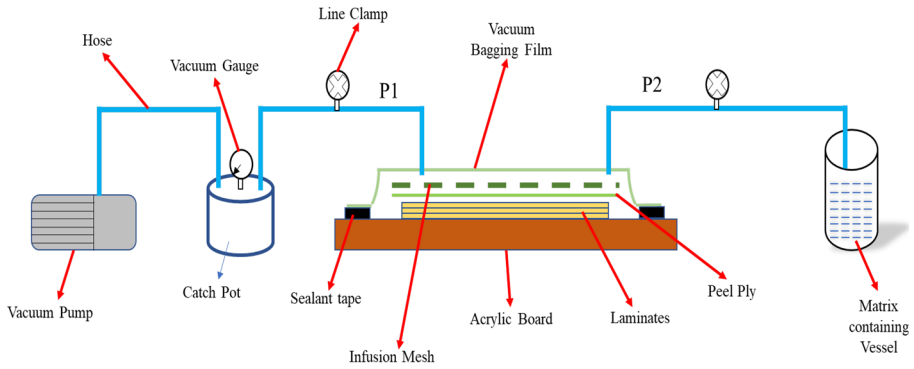


**Fig. 1** Schematic of the Vacuum Infusion Method (VIM)

The details of each composite type for number of layers, stacking sequence and other relevant information related to its fabrication were mentioned in Table 1.

### 3 Drop Weight Impact Test

The drop weight impact test was performed on fabricated basalt and jute-basalt polymer composite laminates to determine the damage resistance and ply level failure using the standard laminate stacking sequence prescribed by ASTM D7136. The impactor had a hemispherical tup shaped geometry made of stainless steel with mass of 5.277 kg. The specimen was placed in the rigid fixture and securely fixed using four screw clamps between upper and lower frame and was subjected to an out-of-plane impact (perpendicular to the plane of the laminate) using a drop-weight device of CEAST 9350 model as shown in Figs. 3 and 4. The machine had a pneumatic clamping with provision of 76.2 mm diameter opening to position the test specimen. It was equipped with anti-rebound mechanism to prevent multiple hits. The force data obtained from output of load cell installed inside the impactor tup was recorded digitally and integrated to obtain the velocity and displacement of the impactor. Impactor mass was kept constant (5.277 kg) and the required impact energy was achieved by dropping the impactor from a pre-calculated height. The change in kinetic energy of the impactor equals the energy absorbed by the target most of which is dissipated in plasticity and damage.

Three samples were tested for each laminate for the conditions specified in Table 2.

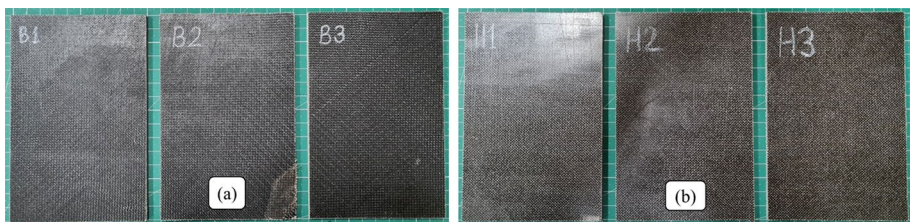


**Fig. 2** Fabricated composite panels of the **a** Basalt (BFRP) and **b** Hybrid (B-JFRP)

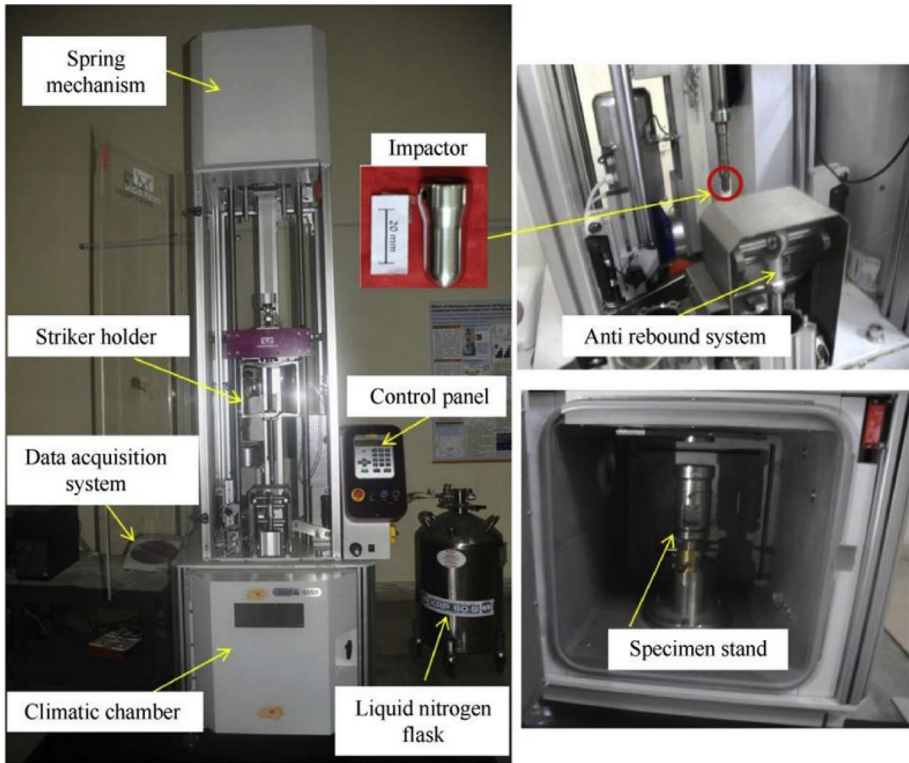


Fig. 3 Drop weight impact tester (CEAST-Instron 9350 model)

### 3.1 Geometrical Modeling and Boundary Conditions

In the FE analysis, the rectangular plate of 150 mm by 100 mm was modeled as 3D deformable type. The lamina element chosen was solid type during the composite layup. The impactor was modeled as a 3D discrete rigid body with a hemispherical shape of diameter of 12.7 mm. The inertia mass of the impactor was assumed to have concentrated at its centre of gravity which was defined by a reference point. To simulate the clamped edges of the laminate, all the edges of the plate are fully fixed (ENCASTRE) with no rotation and was restricted to have displacement only in the impact direction. All the nodes of the plate edge were fixed in all directions (x, y, z) as shown in Fig. 5.

Table 1 Composite laminate fabrication details

Laminate	No. of layers	Lamina thickness (mm)	Stacking sequence (ASTM D7136)	Total thickness, t (mm)
BFRP	28	0.2	$[(+45^\circ/-45^\circ) / (0^\circ/90^\circ)]_{7S}$	5.5
B-JFRP	12	0.7 and 0.2	$\{[(+45^\circ/-45^\circ)_B / (0^\circ/90^\circ)_J]_3 / \{(0^\circ/90^\circ)_B / (+45^\circ/-45^\circ)_J\}_3\}$	5.6

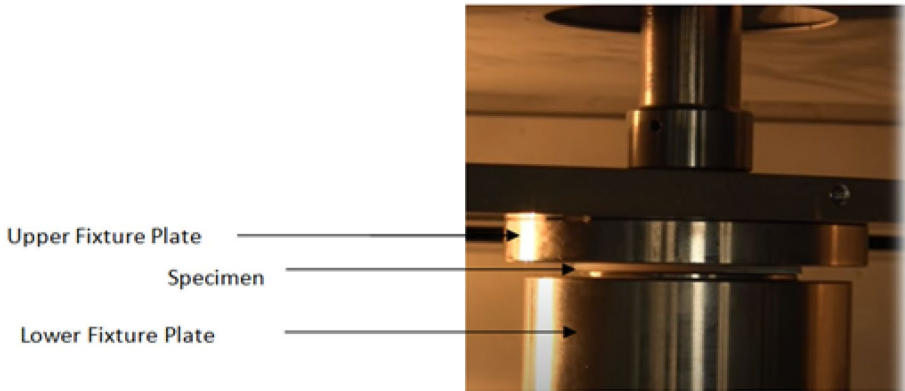


**Fig. 4** Specimen clamped with Fixtures

### 3.2 Finite Element Modeling

A mesh using three dimensional 8-noded brick elements (C3D8R) was done and single element across the thickness was taken in each ply. The optimum mesh size for impact zone (20 mm × 20 mm in the centre of ply) chosen after mesh convergence was 1 mm × 1 mm and coarse mesh in the remaining regions as shown in Fig. 5. This helped reduce the computation time and focus on the impact zone where the impact is concentration. To control element distortion, the damage variable was assigned a value of 0.99 to maintain residual stiffness.

Fiber tension and compression as well as matrix tension stress based Hashin [25] failure criteria were used to model the damage initiation criteria. Matrix compression damage initiation was modeled using the Puck and Shurman [33] criterion because of consider a fracture plane. Damage propagation of fiber and matrix for tension and compression Shi et al. [3] criteria were modeled to accurately prediction of composite failure behavior.

A damage-based constitutive equation was employed to model the unidirectional lamina of composite. Damage initiation criteria  $F_{ij}^k$  (Hashin [25], Puck and Shurman [33]) and damage propagation criteria  $L_{ij}^k$  (Shi et al. [3]) were adopted to account for matrix and fiber failure during the low velocity impact. Failure initiation occurs in the material when some failure criterion  $F_{ij}^k$  was met. Subsequently, the damage growth is leading up

**Table 2** Specifications of impact tests as per ASTM D7136

Impactor mass (kg)	Sample Dimensions (mm)	Impact velocity (m/s)	Energy impacted (J)
5.277	100 × 150 × t	1.947	10
		2.753	20
		3.372	30

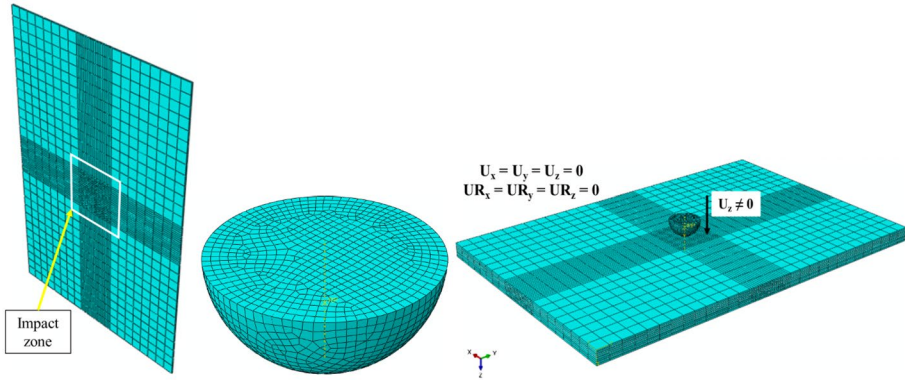


Fig. 5 FE model of lamina, impactor and model assembly

to the final failure of the structure as shown in flow chart Fig. 6. User subroutine was implemented as these features do not exist in commercial software (e.g. ABAQUS) to accurately predict the composite damage response.

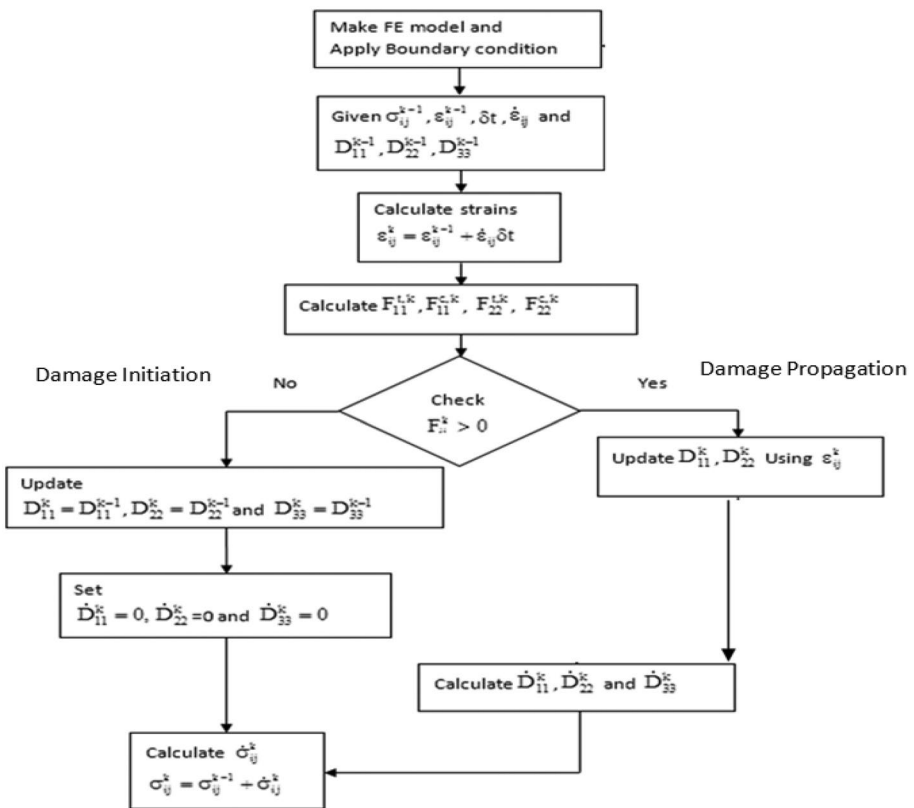


Fig. 6 Flow chart of the user defined subroutine

**Table 3** Elastic and strength properties of JFRP (experimentally obtained) and BFRP

Property	JFRP <sup>a</sup>	BFRP <sup>b</sup>	Property	JFRP <sup>a</sup>	BFRP <sup>b</sup>
E <sub>11</sub> (GPa)	11.38	18.68	ν <sub>13</sub>	0.3	0.3
E <sub>22</sub> (GPa)	11.38	18.68	ρ (kg/m <sup>3</sup> )	1168	1760
E <sub>33</sub> (GPa)	5.64	9.82	S <sub>1t</sub> (MPa)	59.3	360
G <sub>12</sub> (GPa)	2.049	2.8	S <sub>2t</sub> (MPa)	59.3	360
G <sub>23</sub> (GPa)	2.049	2	S <sub>3t</sub> (MPa)	40	40
G <sub>13</sub> (GPa)	1.28	2.8	S <sub>1c</sub> (MPa)	70	200
ν <sub>12</sub>	0.153	0.04	S <sub>2c</sub> (MPa)	40	90
ν <sub>23</sub>	0.153	0.3	S <sub>3c</sub> (MPa)	40	90
G <sub>1c</sub> <sup>T</sup> (kJ/m <sup>2</sup> )	617	2314	G <sub>2c</sub> <sup>T</sup> (kJ/m <sup>2</sup> )	56	91
G <sub>1c</sub> <sup>C</sup> (kJ/m <sup>2</sup> )	700	5600	G <sub>2c</sub> <sup>C</sup> (kJ/m <sup>2</sup> )	86	112

a – Maharshi and Patel [5, 6] b – Gupta et al.[24]

### 3.3 Material Properties

The detailed material properties were listed in Table 3. The composite laminate properties of jute composite were experimentally obtained by Maharshi and Patel [5, 6] and material properties of basalt were taken from Gupta et al. [24].

### 3.4 Contact Algorithm

A general contact algorithm was applied between impactor and laminate plies. The contact algorithm was based on penalty method with hard contact between the impactor and the laminate while a coulomb friction model was used between the laminate plies. A coefficient of friction value of 0.3 was given between the adjacent plies and between the metal impactor and laminate [3].

Delamination modelling of the composite plies cohesive surface modelling was applied using the ABAQUS software. The cohesive surface parameters of elastic modulus and inter laminar strength and toughness have been listed in Table 4 (Shi et al. [3]).

The traction separation behaviour between the composite plies was given by Eq. 1 [3].

$$\left(\frac{t_n}{t_n^0}\right)^2 + \left(\frac{t_s}{t_s^0}\right)^2 + \left(\frac{t_t}{t_t^0}\right)^2 = 1 \tag{1}$$

where,  $t_n^0$ ,  $t_s^0$  and  $t_t^0$  were the maximum contact stresses in normal and two shear directions.  $t_n$ ,  $t_s$  and  $t_t$  are the undamaged stresses in normal and two shear directions. The components of normal and two shear stress vectors are given by,

$$t_n = (1 - d_c)t_n \quad t_s = (1 - d_c)t_s \quad t_t = (1 - d_c)t_t \tag{2}$$

**Table 4** Cohesive parameters used in the interface [3]

Properties	Normal	Shear I	Shear II
Normalized elastic modulus (GPa/mm)	1373.3	493.3	493.3
Inter-laminar strength (MPa)	62.3	92.3	92.3
Interlaminar fracture toughness (J/m <sup>2</sup> )	290	780	780



The estimation of crack propagation is given by the power law in Eq. 3.

$$\left(\frac{G_n}{G_n^c}\right)^\alpha + \left(\frac{G_s}{G_s^c}\right)^\alpha + \left(\frac{G_t}{G_t^c}\right)^\alpha = 1 \quad (3)$$

where,  $G_n$ ,  $G_s$ , and  $G_t$  are work done during traction.  $G_n^c$ ,  $G_s^c$ , and  $G_t^c$  are critical fracture energies in normal and two shear directions. For the prediction of delamination behaviour in composite materials mixed mode decohesion elements were proposed by Shi et al.[3]. A single damage parameter based on relative displacement which could be applied to track the damage state of the interface under any mode interaction was developed. The value of  $\alpha$ , taken to be 1.45, was experimentally obtained using Benzeggagh–Kenane fracture energy law for mixed-mode loading [3].

## 4 Results and Discussion

As mentioned in previous section, composite plates were made from jute and basalt fabrics for impact test as per ASTM D7136. The tests were performed using the drop weight impact tester (CEAST- 9350) for three energy levels. Impactor mass was kept constant (5.277 kg) and required impact energy was achieved by dropping the impactor from a pre-calculated height. The chosen impact energies were 10, 20 and 30 J to cover the range from matrix failure to damage resistance of the fabricated laminates. The corresponding impact velocities were 1.947, 2.753 and 3.372 m/s, respectively. Data acquisition system was used to record the force – time data and impact parameters like peak force, absorbed energy, maximum displacement and impact velocity were calculated using the in-built software of the equipment. The results were also validated by FE simulation using VUMAT sub – routine in ABAQUS/Explicit.

### 4.1 Energy Profile Diagram

Energy profile diagram is a plot of absorbed energy against impact energy which is used to indicate the penetration and perforation threshold energy. Damage analysis of a composite material in the event of an impact test is a complex process as it depends on various factors and boundary conditions. During an impact event, for any material, there are mainly three types of response observed in energy – time graph which are rebounding, penetration and perforation. These responses help to understand the material failure behaviour and stiffness characteristics (whether ductile or brittle). To graphically portray the peak energy response of the impact test, one should draw the energy profile diagram [34] to know how the material behaves during an impact. Energy profile diagram shows absorbed energy magnitude against impact energy and includes equal energy line; an imaginary line which is impact energy equals absorbed energy. Figure 7 shows the energy profile of all three types of samples for three different energy levels.

When the energy of impactor is not enough to infiltrate the test sample, rebounding occurs. Here, impactor gives some of its energy to the sample during surface contact and damages it. This phenomenon reduces the impactor energy and velocity. After a certain time of contact, the velocity of impactor becomes zero and then its motion of direction changes. The energy absorbed in the sample gets converted to damage in the form of fiber and matrix failure or delamination. During the impact test, basalt composite (BFRP) was

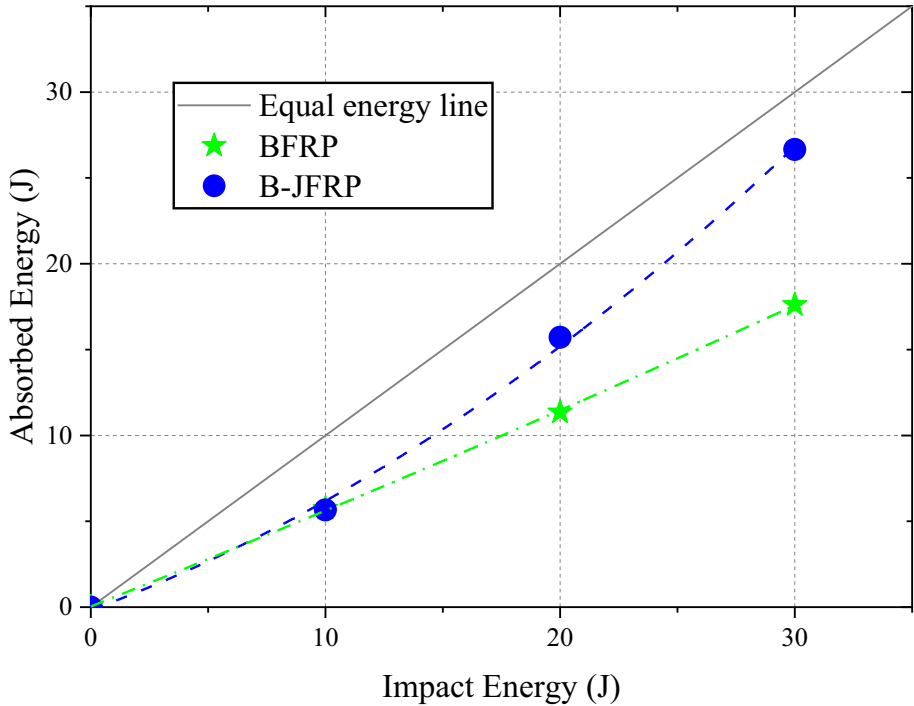
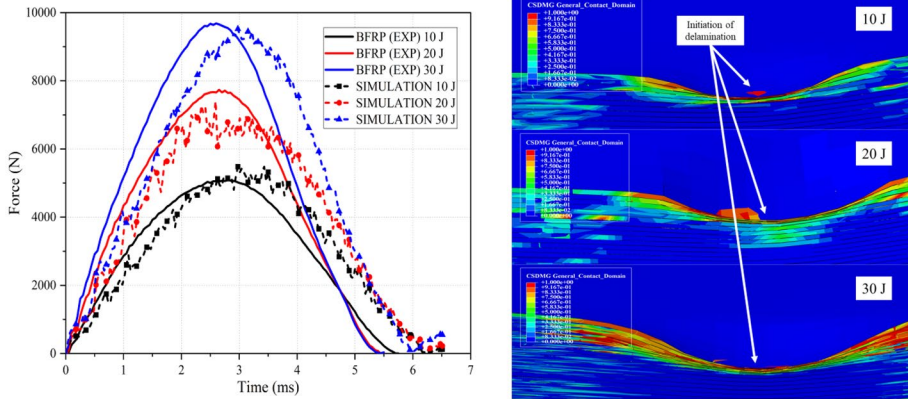


Fig. 7 Equal energy diagram of B-JFRP and BFRP composites

able to absorb energy without having much material damage. This can be seen from the figure as the slope of the curve for BFRP was low. BFRP had damage only in the form of matrix cracking and had no delamination phenomenon. The effect of hybridisation can be clearly seen as basalt fiber improved the impact behaviour of B-JFRP. The low slope angle indicated that damage resistance of the composite had improved and delamination phenomenon was delayed with high energy level. The hybrid composite did not completely perforate at 30 J but partial penetration occurred. This means that the hybrid composite had the capability to absorb more energy before complete failure or perforation.

#### 4.2 Force – Time History

For low impact energies of the order of 1 – 5 J [35], the graphs are generally symmetric around the peak load since the energy absorbed by the specimen does not damage it and remain under elastic region of the material. The force – time curves at low impact energies are symmetrical as the loading and unloading time is nearly equal. However, during the initial contact when the impactor is in loading condition, there are slight oscillations due to elastic vibration. These vibrations are due to the contact between the impactor and the specimen after which the impactor bounces back and the load is reduced to zero. This process indicates the initiation of damage in the composite when matrix failure occurred and cracks are seen.



**Fig. 8** Force – time history of BFRP and image of delamination initiation within the impact zone

Figure 8 shows the load – time history or force – time history of basalt composite samples for three impact energy levels. The BFRP was tested for 10 J, the curve showed symmetry and there was very little elastic vibrations highlighting the excellent strength and resistance to impact. Similarly, the graph had a similar behaviour at 20 J and 30 J with increasing peak load at about the same contact time and duration. The only damage visibly seen was matrix cracking. However, if the simulation results were seen for delamination, it was observed that there was some delamination within the impact zone and it increased with increasing impacting energy.

The force – time history of B-JFRP composite for 10 J had symmetric curve as the laminate was able to withstand the impact with fiber damage as shown in Fig. 9. The loading and unloading time was almost similar with slight elastic vibrations towards the peak force indicating towards damage initiation. At 20 J, there were intense vibrations near the peak force with oscillations at the peak. This was due to progressive fiber damage after matrix cracking and complete failure of matrix system. Jute fiber was unable to bear damage beyond 10 J due to which delamination and fiber breakage was seen

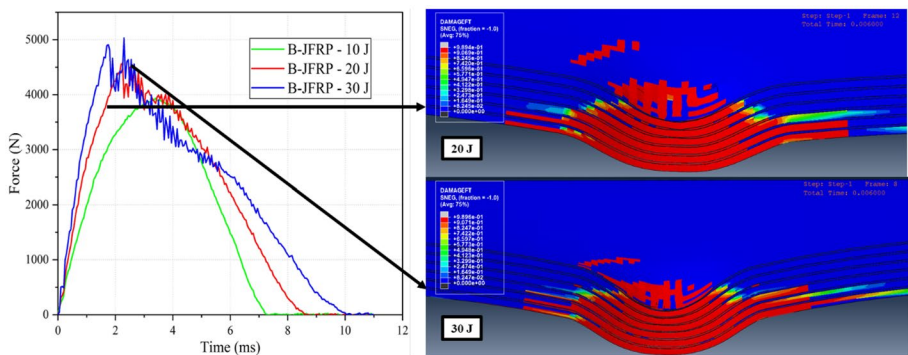


**Fig. 9** Experimental force – time history of B-JFRP and numerical images of fiber damage during the impact

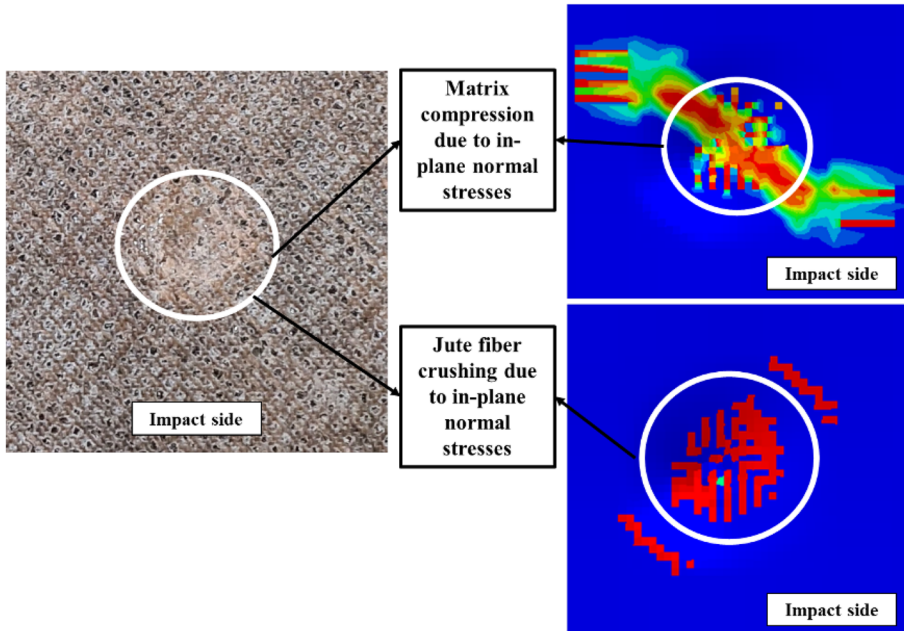
on the back side of the plate; though much of the damage was absorbed by basalt fiber resulting in minimum damage and no penetration. The low shear strength of both fibers resulted in fiber breakage and delamination. At 30 J, there were intense elastic vibrations near the peak and the curve was not symmetric. As the curve reached its peak there were high oscillations in the loading and gradual decrease with time. The peak force oscillations in loading indicated penetration of the impactor with clear delamination seen in the rear. Profound fiber breakage of both the fibers were seen although much of which were of jute fibers as shown in Fig. 10. At higher energy level, the plate was not able to rebound much of the energy and absorbed around 90% of the impacted energy. Since, basalt fiber has excellent toughness properties, there was no catastrophic failure proving the worth of hybridisation; overall toughness of the composite plate was improved which can also be assessed by the tensile property improvement.

### 4.3 Energy – Time History

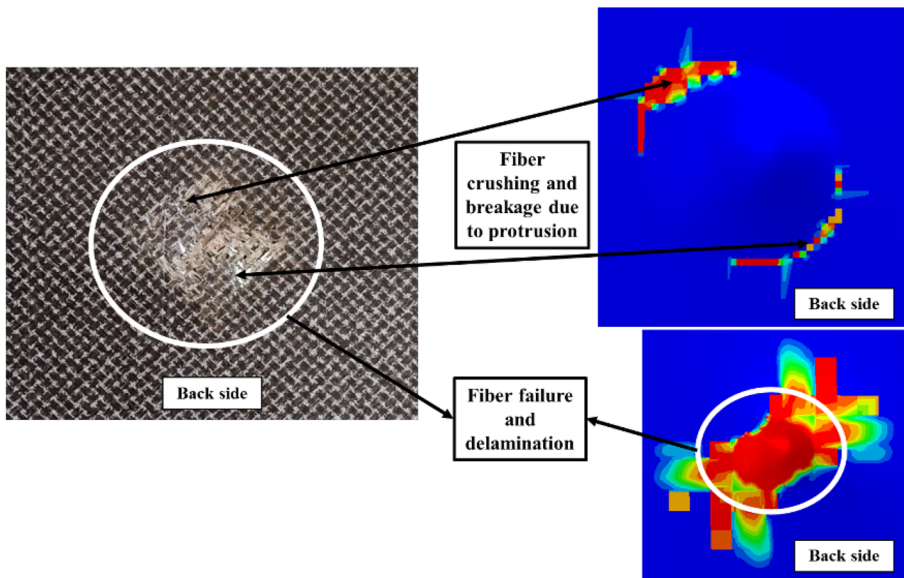
During the impact event, when the impactor makes contact with the composite plate, the initial kinetic energy of the impactor gets transferred to the plate. During this time, a part of the energy is absorbed by the plate in the form elastic deformation (elastic energy) while a major portion of the energy is dissipated in the form of delamination, matrix cracking, fiber failure, intra-laminar damage, friction between the impactor and contacting lamina, among neighbouring plies within the laminate during recovery or energy distribution. The velocity with which the impactor makes contact with laminate becomes zero when the kinetic energy is completely transferred to the laminate. Only after this point, the impactor gets rebound in case, the elastic energy stored in the laminate is transferred back to the impactor; if the elastic energy of the laminate is not sufficient for rebound during higher energy levels, the impactor penetrates or perforates the laminate. Finally, the energy absorbed by the composite laminate reaches a stable value resulting from damage and friction when the contact between impactor and sample is lost [21]. The impact energy – time relationship for the composites is shown in Fig. 11. BFRP showed no sign of major damage at 10, 20 and 30 J energy levels. The high toughness of basalt fiber was responsible for such excellent energy absorption of composite plate. At high energy level of 30 J, matrix cracking was observed with dent on the impact side and slight protrusion on the rear side. The curves of all energies were smooth and uniform. When B-JFRP was tested at 10, 20 and 30 J energy levels, the improvements were clear and the hybrid composite was able to absorb high energies. At low energy level, the sample was able to absorb much of the energy without any visible damage apart from matrix cracking. At high energy levels, delamination and fiber failure can be seen from load – time graph which translated to lower rebound energies observed in the energy – time curves. At 10 J, 5.67 J of energy was absorbed whereas 15.718 J and 26.68 J of energy were absorbed at 20 J and 30 J, respectively.

### 4.4 Displacement – Time and Velocity – Time Histories

During the impact, when the impactor impacts the laminates, the deflection increases in the loading time and deflection rate is positive (slope). It is the contact period for which the impactor damages the composite by moving through it and displacing the material in contact. When the impactor loses all the energy in process and elastic energy stored in the composite sample just about to transfer the energy back to the impactor, maximum



(a)



(b)

**Fig. 10** Comparison between experimental and numerical modeling on a impact side for matrix damage **b** damage on the back side due to compression for B-JFRP at 30 J

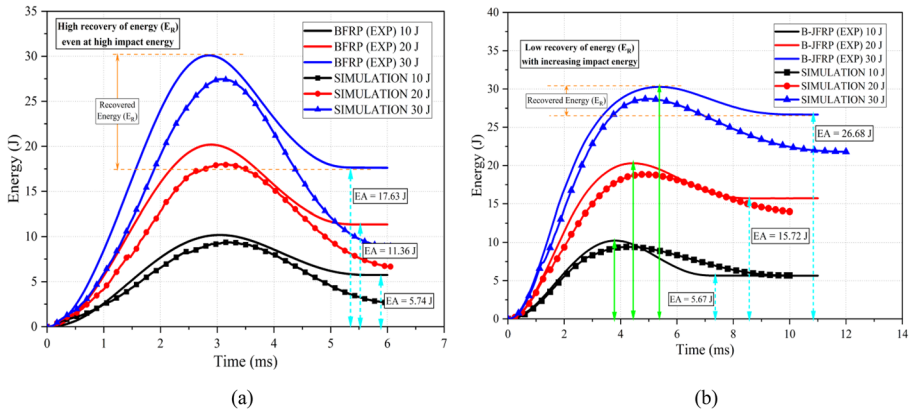


**Fig. 11** Energy – time history of **a** BFRP **b** B-JFRP

deflection in the sample occurs. And when the impactor rebounds, the deflection rate becomes negative as the impactor motion reverses.

The displacement – time graphs of composite laminates for different energy levels are shown in Fig. 12. The maximum deflection in B-JFRP at 10 J was 4.567 mm at 3.8 ms and as mentioned earlier, the maximum energy reached in that moment as well. However, from the force – time graph, it can be seen that the time to attain peak force of 3935.57 N was 3.4 ms which is earlier. Studies have shown that the whole impact event is divided into two durations; impact and rebound durations. The time that divides these durations is the point where the impactor velocity reduces to zero and motion is reversed [21]. During the low energy impacts (1 – 10 J) when the impacts are mostly elastic and no visible damage is seen, the force – time responses are generally symmetric. But in actual cases, plasticity accompanied with damage in different forms lead to the delay in rebound phenomenon as compared to the time to achieve peak force. Thus, in most of the cases, peak force was achieved in the loading region or impact durations and thus energy or displacement curves were delayed as shown in Fig. 13. This delay

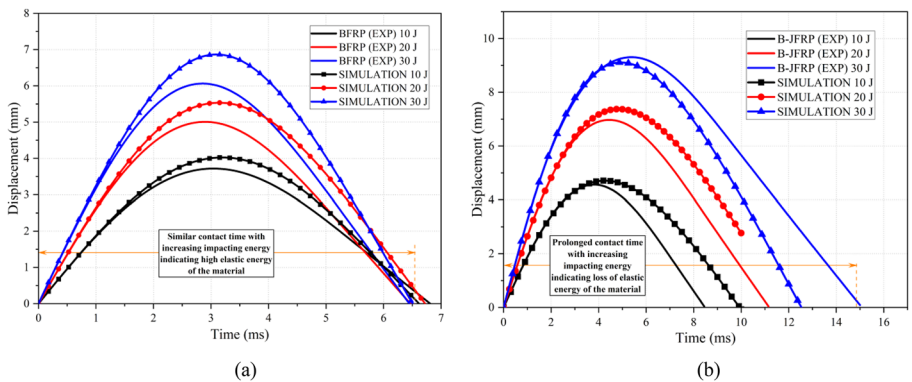


**Fig. 12** Displacement – time history of **a** BFRP **b** B-JFRP

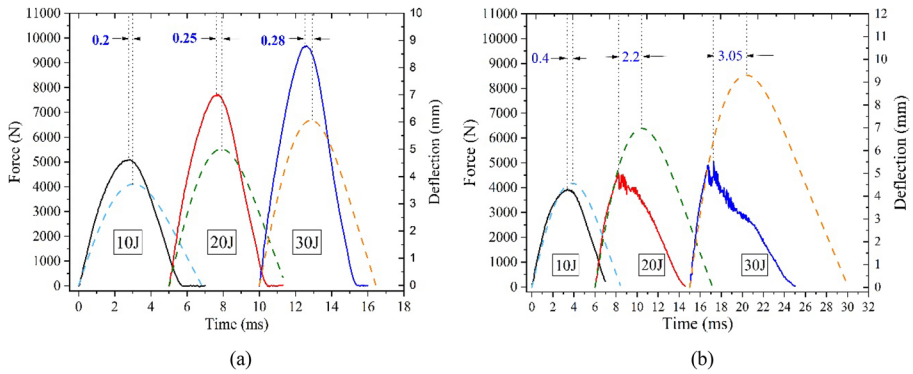


**Fig. 13** Force – time and deflection – time plots for **a** BFRP **b** B-JFRP composite laminates at 10 J, 20 J and 30 J. (solid lines show force data while dotted lines show deflection data)

increased with increase in the impact energy levels since at higher energies, different failure modes will come into picture further delaying rebounding. At 20 J and 30 J energies, the delay for B-JFRP increased to 2.2 ms and 3.05 ms compared to 0.4 ms at 10 J, showing the time for which the impactor was in contact with the laminate and damaging for that period. In case of BFRP, the peak deflection at 10 J was 3.72 mm at 3.05 ms and the time at which peak deflection occurred at 20 J and 30 J was around the same highlighting high elastic energy stored in the laminate to resist the contact time and damage. Also, the delay between peak force and deflection was almost constant corroborating the statement made.

### 4.5 Force – Displacement History

The force – displacement graphs of composite laminates for different energy levels are shown in Fig. 14. The curves give us an interesting overview of the amount of energy utilised at different phases of time (time durations explained in Sects. 4.2 and 4.4). Generally,

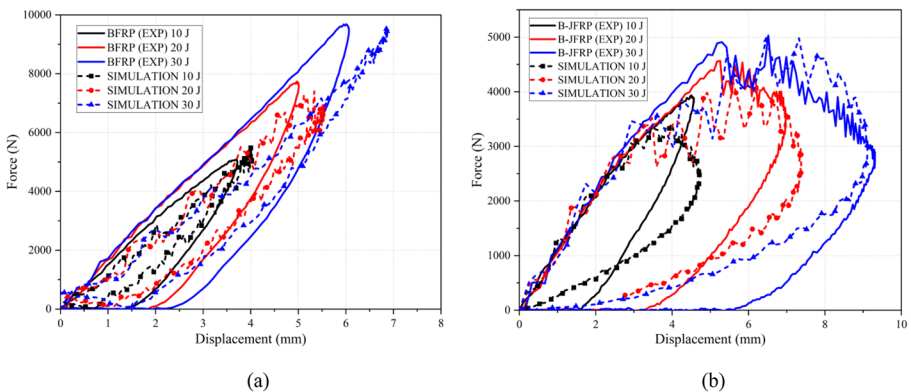


**Fig. 14** Force – displacement history of **a** BFRP **b** B-JFRP

the curves exhibit two types, closed type when rebounding occurs with minimum damage and open type which is characterised by excessive damage or complete failure [34]. Closed types of curve represent the elastic responses of an impact event occurring generally at low energy levels. There is an ascending and a descending section in a closed type of curve in which the ascending includes impact loading region whereas descending is a combination of loading and unloading phases. It is the descending part which shows the impact response of a material. The area inside the loop is the energy dissipated due to plastic deformation and damage. The closed form suggests that complete perforation of plate did not occur and the impactor rebounded with the left-over strain energy in the plate imparted to it [23]. When the material is penetrated or perforated during the impact, the curve does not close and the descending phase does not pass through origin or reverts to original state. The force – displacement graphs for B-JFRP composite presented the scenario where effects of both materials can be observed. Hertzian effect [21] was also seen in these composite laminates. The hybrid composite was able to have closed loop curve at 10 J where elastic energies were observed to play the part. However, when impact energy was 20 and 30 J, due to low impact strength of jute fibers compared to basalt fibers, the laminate had intense vibrations near the peak load highlighting onset of delamination, fiber breakage and failure among the neighbouring plies of jute fibers and sudden transfer of load to the basalt fibers. Because of high toughness of basalt fibers, it was able to recover with a protruding hemispherical dome shape at the opposite side of impact leading to a sudden rise in absorbed energy. The area under the closed loop curve increased with increasing impacting energy highlighting the severity in composite damage before recovery and complete failure.

BFRP on the other hand, was able to keep the damage at bay due to high toughness and strength [10, 11]. The initial slopes at all energy levels were similar with sharp rebounding phase indicating a strong response of the material at those energies [34]. The small disturbances in the force values during the initial phase could be Hertzian failure which denotes the initiation of damage in the form of interlaminar delamination. There was visibly no severe damage in the tested sample with minor depression on the impact side at 30 J indicating onset of matrix cracking. This was also seen from the energy profile where the slope of the curve was almost linear.

#### 4.6 Damage Morphology

Different modes of failure occur during the impact test and visual inspection of the damaged laminates show different modes such as surface micro cracks, indentations, interface delamination, debonding, matrix cracking, fiber breakage, fiber pull out and ply level failure among neighbouring plies [21]. Matrix cracking is the most common phenomenon due to through thickness shear stresses that happened in every sample since the strength of epoxy is lower compared to both the fibers.

Visual inspection of B-JFRP laminates in Figs. 9 and 10 show damage based on impacting energy and material properties. At 10 J, matrix cracking was observed with no visible major damage and a slight depression on the impacting side. At 20 J, the sample showed delamination and fiber breakage with small dome shaped protrusion on the rear side. Delamination occurred due to low bonding strength between the two fibers and low jute fiber strength in general. Through thickness shear stresses at high energy levels caused severe damage and propagate through lower plies. There was visible fiber breakage at the rear side but there was no perforation. Similar observation was made at 30 J with more intense damage happening at front and back side. The dome shaped protrusion was even



**Fig. 15** CT scans of BFRP samples from **a** Impact side of 20 J **b** 30 J impacted laminates showing impact and non-impact side damaged areas

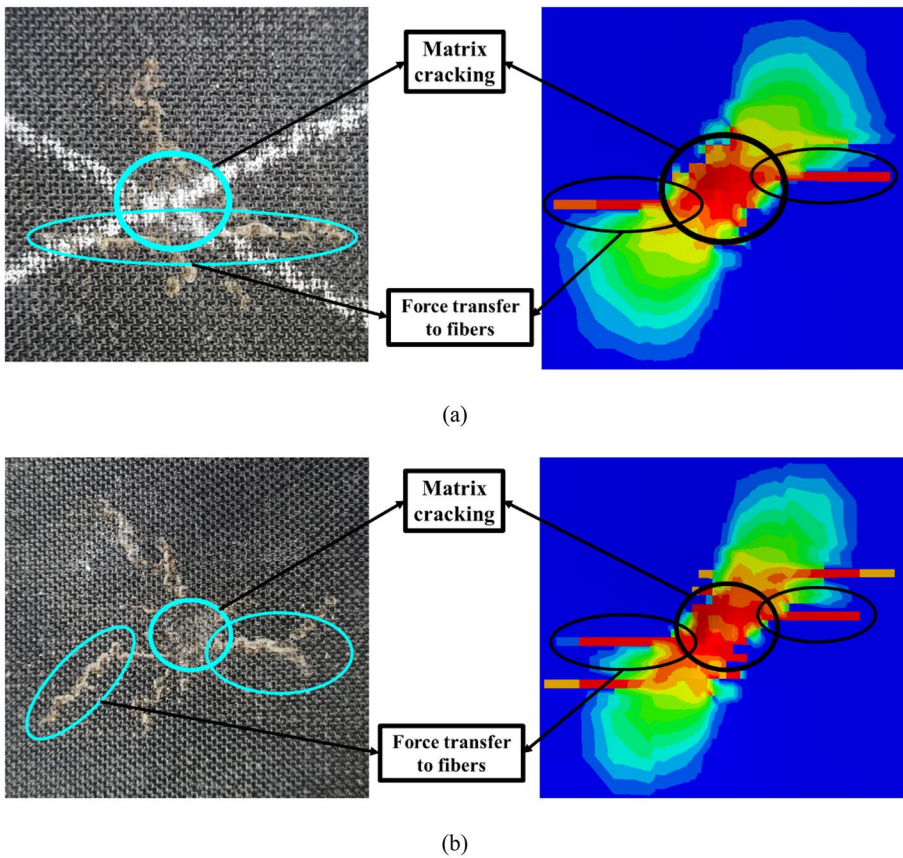
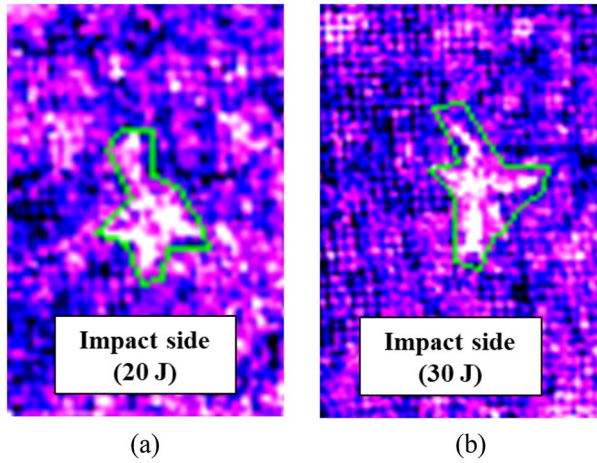


**Fig. 16** Comparison between experimental and numerical modeling on impact side for matrix damage **a** 20 J **b** 30 J due to compression for BFRP

bigger with severe fiber damage but basalt fiber high toughness was able to subdue the perforation at 30 J. These fiber damage and delamination at the rear side can be interpreted from force – displacement curve as well where intense oscillations were seen near the peak loading and major recovery of the laminate.

BFRP on the other hand, bear no major damage at any energy level except for matrix cracking at high energy levels. The damage was local and it did not propagate in the laminate. At high energy level, slight delamination with the immediate ply beneath can be interpreted from the simulation but overall, there was no clear indication.

The images of the sample were not able to capture any detail with clarity to understand any failure happening. So, CT-Scan of the samples was done to see for any external or internal damage. The image of the scans is shown in Fig. 15. BFRP laminate impacted for 10 J showed no damage indicating good interface property and high energy absorption capability of the basalt fibers. At 20 and 30 J, scans were able to detect damage due to matrix cracking (highlighted as white spot in green enclosure) which can also be seen in Fig. 16 but there was no sign of delamination within the top plies and no visible damage on the rear side.

## 5 Conclusions

The current study was focussed on the impact response and impact induced damage for composite laminates made of jute and basalt fibers that were investigated experimentally and numerically under different impact energy levels of 10 J, 20 J and 30 J. The impact test was performed for various impact parameters like peak force, maximum displacement, absorbed energy and damaged area. The numerical validation was performed using VUMAT subroutine in ABAQUS/Explicit to predict the realistic failure fiber, matrix and delamination.

- The peak force of B-JFRP was improved due to hybridisation and the damage resistance of it could be seen as the impactor was unable to fully perforate at 30 J. The same could be validated through simulation where last few layers resisted complete penetration.
- The alternating stacking sequence was successful in minimising the use of basalt and enhancing the overall performance of the hybrid composite.
- The hybrid composite had low recovery at high energy level highlighting irrecoverable damage with fiber and matrix failure (visibly seen) and delamination (simulation). In comparison to basalt composite, the recovery was high indicating high resistance to deformation. Thus, the use of basalt fabric can be seen to improve the damage resistance and energy absorption capability.
- The time to reach peak impact energy and maximum displacement was same in both the composite which was also validated in simulation but the peak force reached earlier at all the impacting energy level and this time gap increased with increasing energies. This indicated the vulnerability at high energy level as the contact time of impactor with the laminate was high prolonging the damage.

**Acknowledgements** The authors would like to thank Dr. Atul R. Bhagat, Head of the composite lab at DRDL Imarat, Hyderabad, for his support in allowing them to perform the tests.

**Author Contributions** Kumar Maharshi: Writing - original draft, Visualization, Formal analysis, Investigation, Software, Conceptualization, Methodology, Validation, Investigation, Conceptualization, Methodology. Shivdayal Patel: Writing - Review & editing, Resources, Conceptualization, Methodology, Supervision, Software.

**Data Availability** No datasets were generated or analysed during the current study.

## Declarations

**Competing Interests** The authors declare no competing interests.

## References

1. Nurazzi N. M., Asyraf M. R. M., Khalina A., Abdullah N., Aisyah H. A., Rafiqah S. A., Sabaruddin F. A., Kamarudin S. H., Norrahim M. N. F., Ilyas R. A. and Sapuan S. M.: A Review on Natural Fiber Reinforced Polymer Composite for Bullet Proof and Ballistic Applications. *Polymers*. **13**(4), 646 (2021)
2. Thomason J. L. and Rudeiros-Fernández J. L.: A Review of the Impact Performance of Natural Fiber Thermoplastic Composites. *Front. Mater.* **5**(60), 1–18 (2018)
3. Shi, Y., Swait, T., Soutis, C.: Modelling damage evolution in composite laminates subjected to low velocity impact. *Compos. Struct.* **94**(9), 2902–2913 (2012)
4. Pathak, R.K., Patel, S., Gupta, V.K.: A Computational Analysis of the High-velocity Impact Performance of Lightweight 3D Hybrid Composite Armors. *Appl. Compos. Mater.* **30**, 727–751 (2023). <https://doi.org/10.1007/s10443-023-10112-0>
5. Maharshi, K., Patel, S.: Experimental Statistical Analysis of Tensile and Shear Properties of the Jute Fabric Epoxy Composites. *J. Nat. Fibers*. 8714–8726 (2021)
6. Maharshi, K., Patel, S.: A study of the Flexural Properties of Jute Fabric Reinforced Epoxy Composite: Experimental and Uncertainty Analysis. *J. Nat. Fibers*. 14654–14665 (2022)
7. Ramesh M., Palanikumar K. and Reddy K. H.: Mechanical property evaluation of sisal–jute– glass fiber reinforced polyester composites. *Composites: Part B*. **48**, 1–9 (2013)
8. Bandaru, A.K., Patel, S., Sachan, Y., Ahmad, S., Alagirusamy, R., Bhatnagar, N.: Mechanical characterization of 3D angle-interlock Kevlar/basalt reinforced polypropylene composites. *Polym Test.* **55**, Pages 238–246, 2016.
9. Bandaru, A.K., Patel, S., Ahmad, S., Bhatnagar, N.: An experimental and numerical investigation on the low-velocity impact response of thermoplastic hybrid composites. *J. Compos. Mater.* **52**, 877–889 (2018)
10. Amuthakkannan, P., Manikandan, V., Jappes, J.T.W., Uthayakumar, M.: Influence of stacking sequence on mechanical properties of basalt-jute fiber-reinforced polymer hybrid composites. *J. Polym. Eng.* **32**, 547–554 (2012)
11. Amuthakkannan, P., Manikandan, V., Jappes, J.T.W., Uthayakumar, M.: Hybridization effect on mechanical properties of short basalt/jute fiber-reinforced polyester composites. *Sci. Eng. Compos. Mater.* **20**(4), 343–350 (2013)
12. Fiore, V., Scalici, T., Badagliacco, D., Enea, D., Alaimo, G., Valenza, A.: Aging resistance of bioepoxy jute-basalt hybrid composites as novel multilayer structures for cladding. *Compos. Struct.* **160**, 1319–1328 (2017)
13. Fiore, V., Scalici, T., Sarasini, F., Tirillo, J., Calagbrese, L.: Salt-fog spray aging of jute-basalt reinforced hybrid structures: Flexural and low velocity impact response. *Compos. B* **116**, 99–112 (2017)
14. Zareei, N., Geranmayeh, A., Eslami-Farsani, R.: Interlaminar shear strength and tensile properties of environmentally-friendly fiber metal laminates reinforced by hybrid basalt and jute fibers. *Polym. Testing* **75**, 205–212 (2019)
15. Lopresto V., Leone C. and Iorio I. D.: Mechanical characterisation of basalt fibre reinforced plastic. *Composites: Part B*. **42**, 717–723 (2011)
16. Scalici, T., Pitarresi, G., Badagliacco, D., Fiore, V., Valenza, A.: Mechanical properties of basalt fiber reinforced composites manufactured with different vacuum assisted impregnation techniques. *Compos. B* **104**, 35–43 (2016)
17. Sapuan S. M., Aulia H. S., Ilyas R. A., Atiqah A., Dele-Afolabi T. T., Nurazzi M. N., Supian A. B. M. and Atikah M. S. N.: Mechanical Properties of Longitudinal Basalt/Woven-GlassFiber-reinforced Unsaturated Polyester-Resin Hybrid Composites. *Polymers* **12**(10), 2211 (2020)
18. Ricciardi, M.R., Papa, I., Lopresto, V., Langella, A., Antonucci, V.: Effect of hybridization on the impact properties of flax/basalt epoxy composites: Influence of the stacking sequence. *Compos. Struct.* **214**, 476–485 (2019)

19. Patel, S., Ahmad, S.: Probabilistic failure of graphite epoxy composite plates due to low velocity impact. *ASME J. Mech. Des.* **139**(4), 044501 (2017)
20. Patel, S., Ahmad, S., Mahajan, P.: Safety assessment of composite beam under ballistic impact. *Thin Walled Struct.* **126**, 162–170 (2018)
21. Patel, S., Soares, G.C.: System probability of failure and sensitivity analyses of composite plates under low velocity impact. *Compos. Struct.* **180**, 1022–1031 (2017)
22. Bandaru, A.K., Patel, S., Sachan, Y., Alagirusamy, R., Bhatnagar, N., Ahmad, S.: Low velocity impact response of 3D angle-interlock Kevlar/basalt reinforced polypropylene composites. *Mater. Des.* **105**, 323–332 (2016)
23. Bandaru, A.K., Patel, S., Sachan, Y., Ahmad, S., Alagirusamy, R., Bhatnagar, N.: Mechanical behavior of Kevlar/basalt reinforced polypropylene composites. *Compos. Part A Appl. Sci. Manuf.* **90**, 642–652 (2016)
24. Gupta, M., Singh, H., Khan, A.N., Mahajan, P., Prabhakaran, R.T.D., Alagirusamy, R.: An improved orthotropic elasto-plastic damage model for plain woven composites. *Thin-Walled Structures* **162**, 107598 (2021)
25. Hashin, Z.: Failure criteria for unidirectional fiber composites. *J. Appl. Mech.* **47**, 329–334 (1980)
26. Gupta M., Prabhakaran R.T.D., Mahajan P.: Non-linear material characterization and numerical modeling of cross-ply basalt/epoxy laminate under low velocity impact. *Polym. Test.* **84**, 106349 (2020)
27. Prabhakaran, R.T.D., Gupta, M., Mahajan, P., Ormondroyd, G.A.: Modelling and simulation of natural fibre/epoxy composites – prediction of stress state and deformations. *Int. J. Materials Engineering Innovation* **10**(2), 114–134 (2019)
28. Nayak, S.Y., Sultan, M.T.H., Shenoy, S.B., Kini, C.R., Samant, R., Shah, A.U.M., Amuthakannan, P.: Potential of Natural Fibers in Composites for Ballistic Applications – A Review. *Journal of Natural Fibers* **19**(5), 1648–1658 (2022)
29. Rajole, S., Ravishankar, K.S., Kulkarni, S.M.: Performance study of jute-epoxy composites/sandwiches under normal ballistic impact. *Defence Technology* **16**, 947–955 (2020)
30. Sarasini F., Tirillò J., Valente M., Valente T., Cioffi S., Iannace S. and Sorrentino L., “Effect of basalt fiber hybridization on the impact behavior under low impact velocity of glass/basalt woven fabric/epoxy resin composites. *Composites: Part A*, vol. 47, Pages 109–123, 2013.
31. ASTM D7136/D7136M – 12. Standard Test Method for Measuring the Damage Resistance of a Fiber-Reinforced Polymer Matrix Composite to a Drop-Weight Impact Event. Philadelphia: American Society for Testing and Materials, 2012
32. Reddy, T.S., Reddy, P.R.S., Madhu, V.: Low velocity impact studies of E-glass/epoxy composite laminates at different thicknesses and temperatures. *Defence Technology* **15**, 897–904 (2019)
33. Puck, A., Schurmann, H.: Failure analysis of FRP laminates by means of physically based phenomenological models. *Compos. Sci. Technol.* **58**(10), 1045–1067 (1998)
34. Shishevan F. A., Akbulut H. and Mohtadi-Bonab M. A.: Low Velocity Impact Behavior of Basalt Fiber-Reinforced Polymer Composites. *J. Mater. Eng. Perform.* **26**(6), 2890–2900 (2017)
35. Richardson, M.O.W., Wisheart, M.J.: Review of low-velocity impact properties of composite materials. *Compos. A* **27A**, 1123–1131 (1996)

**Publisher's Note** Springer Nature remains neutral with regard to jurisdictional claims in published maps and institutional affiliations.

Springer Nature or its licensor (e.g. a society or other partner) holds exclusive rights to this article under a publishing agreement with the author(s) or other rightsholder(s); author self-archiving of the accepted manuscript version of this article is solely governed by the terms of such publishing agreement and applicable law.